Author Manuscript

Author Manuscript

Author Manuscript

Author Manuscript

HHS Public Access

Author manuscript

Biochemistry. Author manuscript; available in PMC 2019 April 11.

Published in final edited form as:

Biochemistry. 2018 October 02; 57(39): 5706–5714. doi:10.1021/acs.biochem.8b00784.

Kinetic Understanding of N_2 Reduction versus H_2 Evolution at the E_4(4H) Janus State in the Three Nitrogenases

Derek F. Harris[†], **Zhi-Yong Yang**[†], **Dennis R. Dean**[‡], **Lance C. Seefeldt**[*,†], and **Brian M. Hoffman**[*,§]

[†]Department of Chemistry and Biochemistry, Utah State University, Logan, Utah 84322, United States

[‡]Department of Biochemistry, Virginia Tech, Blacksburg, Virginia 24061, United States

[§]Department of Chemistry, Northwestern University, Evanston, Illinois 60208, United States

Abstract

The enzyme nitrogenase catalyzes the reduction of N_2 to ammonia but also that of protons to H_2. These reactions compete at the mechanistically central 'Janus' intermediate, denoted E_4(4H), which has accumulated $4e^-/4H^+$ as two bridging Fe-H—Fe hydrides on the active-site cofactor. This state can lose e^-/H^+ by hydride protonolysis (HP) or become activated by reductive elimination (*re*) of the two hydrides and bind N_2 with H_2 loss, yielding an E_4(2N2H) state that goes on to generate two NH_3 molecules. Thus, E_4(4H) represents the key branch point for these competing reactions. Here, we present a steady-state kinetic analysis that precisely describes this competition. The analysis demonstrates that steady-state, high-electron flux turnover overwhelmingly populates the E_4 states at the expense of less reduced states, quenching HP at those states. The ratio of rate constants for E_4(4H) hydride protonolysis (k_{HP}) versus reductive elimination (k_{re}) provides a sensitive measure of competition between these two processes and thus is a central parameter of nitrogenase catalysis. Analysis of measurements with the three nitrogenase variants (Mo-nitrogenase, V-nitrogenase, and Fe-nitrogenase) reveals that at a fixed N_2 pressure their tendency to productively react with N_2 to produce two NH_3 molecules and an accompanying H_2, rather than diverting electrons to the side reaction, HP production of H_2, decreases with their ratio of rate constants, k_{re}/k_{HP}: Mo-nitrogenase, 5.1 atm^{-1}; V-nitrogenase, 2 atm^{-1}; and Fe-nitrogenase, 0.77 atm^{-1} (namely, in a 1:0.39:0.15 ratio). Moreover, the lower catalytic effectiveness of the alternative nitrogenases, with more H_2 production side reaction, is not caused by a higher k_{HP} but by a significantly lower k_{re}.

Graphical Abstract

[*]**Corresponding Authors** bmh@northwestern.edu. Phone: +1-847-491-3104. lance.seefeldt@usu.edu. Phone: +1-435-797-3964.

The authors declare no competing financial interest.

ASSOCIATED CONTENT

Supporting Information

The Supporting Information is available free of charge on the ACS Publications website at DOI: 10.1021/acs.biochem.8b00784.

Rate equations for steady-state kinetic analysis of scheme D, H_2 *oa* and the steady-state kinetics, and data for Figures 4–6 and Table 1 (PDF)

Author Manuscript Author Manuscript Author Manuscript Author Manuscript

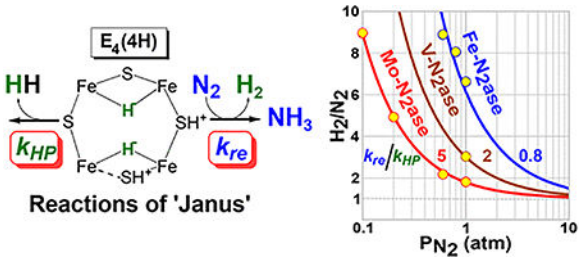

Nitrogenase is the bacterial enzyme responsible for biological nitrogen fixation, the reduction of N_2 to two NH_3 molecules.[1–3] There are three known forms of nitrogenase, designated as the molybdenum-dependent Mo-nitrogenase, the vanadium-dependent V-nitrogenase, and the iron-only Fe-nitrogenase, each encoded by a unique gene cluster.[4–8] Each nitrogenase comprises an electron-delivery Fe protein and a catalytic protein, the latter being denoted MoFe protein (MoFe), VFe protein (VFe), and FeFe protein (FeFe), respectively. Each catalytic protein contains a complex metal cluster called the FeMo-cofactor (FeMo-co), FeV-cofactor (FeV-co), and FeFe-cofactor (FeFe-co), as the active site for substrate reduction.[4,5,9–12] A structural representation of the FeMo-co in the resting state is shown in Figure 1. A recent structure of the VFe protein shows that the FeV-co has a structure similar to that of the FeMo-co but has V replacing Mo and one bridging S replaced by a carbonate.[13] No structure is available for the FeFe-co, but available spectroscopic signatures indicate that the overall structure is similar to those of the FeMo-co and FeV-co.[11]

Mo-nitrogenase is the best characterized of the three nitrogenase forms. During catalysis, the Fe protein transiently associates with the MoFe protein, donating a single electron to the FeMo-co during association, mediated by an [8Fe-7S] cluster (P-cluster).[9,14–16] Each electron delivery is coupled to the hydrolysis of two molecules of ATP by the Fe protein, the P_i release of which is known to be the overall rate-limiting step of catalysis.[17] Studies of the enzyme trapped during catalysis have shown how electrons and protons accumulate on the FeMo-co and how the enzyme is activated for N_2 binding and reduction.[9,18–20] In short, before N_2 can be reduced, four electrons and protons must accumulate on the FeMo-co to create a state denoted $E_4(4H)$, which stores these reducing equivalents as two Fe–H–Fe bridging hydrides. Recent structural and theoretical studies reveal that accumulation of electrons and protons on the FeMo-co can break one or both of the Fe–S–Fe bonds for a "belt" sulfide, thus opening coordination sites for binding of the hydrides to Fe atoms.[13,21–24] These hydrides can produce H_2 through two different reactions (Figure 2). Protonolysis of one hydride (HP) results in the formation of H_2 and the "relaxation" of the $E_4(4H)$ state back to the $E_2(2H)$ state; HP of the second hydride then generates E_0. In competition with HP at $E_4(4H)$ is the reductive elimination (*re*) of both hydrides to make H_2, which is released upon N_2 binding, in a process that leads to a diazene-level complex [$E_4(2N2H)$]. Two molecules of NH_3 are then generated through addition of four additional electrons/protons. As shown in Figure 2, the activation for catalysis by *re* of H_2 is reversible, with the oxidative addition (*oa*) of H_2 by $E_4(2N2H)$ leading to N_2 release.[9,18–21,25] As a result of the mechanistically required release of H_2 for enzyme activation, the *re/oa* equilibrium incorporates an "eight-electron" limiting stoichiometry (eq 1) for N_2 reduction[19]

Author Manuscript Author Manuscript Author Manuscript Author Manuscript

$$N_2 + 8H^+ + 16MgATP + 8e^- \rightarrow 2NH_3 + H_2 + 16MgADP + 16P_i \quad (1)$$

as proposed by Lowe and Thorneley.[26,27] This limiting stoichiometry is, in fact, approached under high N_2 pressures.[28]

Recent studies indicate that all three nitrogenases follow a similar *re/oa* mechanism of nitrogen fixation.[29] However, compared to the Mo-nitrogenase, the V- and Fe-nitrogenases exhibit significant differences in the relative rates of the two reaction pathways, H_2 formation and N_2 reduction. For example, under a 1 atm partial pressure of N_2 [$P(N_2)$], the observed ratio of H_2 formed per N_2 reduced for Fe-nitrogenase is ~7, whereas it is ~3 for V-nitrogenase and ~2 for Mo-nitrogenase.[4,21,29–31]

The stoichiometry of eq 1 was incorporated into a detailed kinetic scheme for the Mo-nitrogenase from the bacterium *Klebsiella pneumoniae* painstakingly developed by Lowe, Thorneley, and others (here termed the LT scheme).[27] Although this scheme provides a framework for mechanistic studies of nitrogenase, the inclusion of all the steps in the complete catalytic cycle of nitrogen fixation came at the cost of significant uncertainties in key rate constants, in particular those associated with reactions of the critical $E_4(4H)$ intermediate.[32] As a consequence, it is not feasible to obtain the large number of variables associated with this model with sufficient precision to use the model to compare the alternative nitrogenases.

To gain a precise description of the reactions at the $E_4(4H)$ state of the three nitrogenases, we have developed a kinetic description of steady-state turnover that optimally provides an analysis of the competing reactions of this ‘Janus’ intermediate.[9] It focuses on the competition between progress toward NH_3 formation through N_2 binding/H_2 *re* to generate $E_4(2N2H)$ and the relaxation toward the resting state by H_2 formation through HP (Figure 2). Application of this kinetic model to measurements of turnover of catalysis by the three nitrogenases provides quantitative comparisons of the catalytic behavior of their Janus intermediates and critical insights into the differences in their reactivity.

MATERIALS AND METHODS

Reagents and General Procedures.

All reagents were obtained from Sigma-Aldrich (St. Louis, MO), Fisher Scientific (Fair Lawn, NJ), or Bio-Rad (Hercules, CA) unless specified otherwise and used without further purification. Argon and dinitrogen gases were purchased from Air Liquide America Specialty Gases LLC (Plumsteadville, PA). Proteins and buffers were manipulated anaerobically in septum-sealed serum vials and flasks using a vacuum Schlenk line, an argon or dinitrogen atmosphere, and gastight syringes. Gas transfers were made using gastight syringes.

Author Manuscript Author Manuscript Author Manuscript Author Manuscript

Bacterial Growth and Protein Purification.

Fe-nitro- genase proteins (FeFe and Fe protein) were expressed and purified from *Azotobacter vinelandii* strain DJ1255 as previously described.[29] Mo-nitrogenase proteins (MoFe and Fe proteins) were expressed and purified from *A. vinelandii* strains DJ995 (His-MoFe protein) and DJ884 (Fe protein) as previously described.[33–35] Protein concentrations were determined using the Bio-Rad DC Protein Assay Kit.

Proton and Dinitrogen Reduction Assays.

Substrate reduction assays were performed in 9.4 mL serum vials containing a MgATP regeneration buffer (6.7 mM $MgCl_2$, 30 mM phosphocreatine, 5 mM ATP, 0.2 mg/mL creatine phosphokinase, and 1.2 mg/mL BSA) and 10 mM sodium dithionite in 100 mM MOPS buffer at pH 7.0. Reaction vials were made anaerobic, and their headspaces adjusted to the partial pressure of N_2 desired with the remaining headspace consisting of argon. The FeFe or MoFe protein was then added to the vials; the vials were vented to atmospheric pressure, and the reactions were initiated by the addition of the appropriate Fe protein. FeFe and MoFe concentrations in reactions were 0.1 mg/mL, corresponding to ~0.42 and ~0.4 nmol, respectively, per reaction vial. All data reported here were collected at a 1:30 FeFe:Fe protein molar ratio and a 1:20 MoFe:Fe protein molar ratio, except in a series of measurements designed to test the specific activity as a function of the electron flux, which is controlled by this ratio. Reactions were conducted at 30 °C for 8 min and then stopped by the addition of 300 μ*L* of 400 mM EDTA (pH 8.0). To minimize the effects of slow re-reduction of Fe protein by sodium dithionite under low-flux conditions (high ratio of MoFe protein to Fe protein), The flux dependence of N_2 reduction by Mo-nitrogenase employed a buffer containing a MgATP regeneration system (5 mM $MgCl_2$, 22 mM phosphocreatine, 3.8 mM ATP, 0.15 mg/mL creatine phosphokinase, and 0.8 mg/mL BSA) with 0.125 mM 1,4-dithiothreitol, 0.6 mM flavodoxin in the hydroquinone state (Fld^{HQ}), and 12 mM sodium dithionite in 100 mM MOPS at pH 7.3. The Fe protein concentration was fixed at 0.1 mg/mL, and the MoFe protein concentration was varied from 0.2 to 6.4 mg/mL to give a [MoFe]:[Fe] ratio from 0.5 to 16. The reaction mixtures were incubated at 30 °C for 30 s under 1 atm of N_2, and then the reactions were stopped by the addition of 500 μ*L* of 400 mM EDTA at pH 8.0. H_2 and NH_3 were quantitated according to published methods.[36,37]

Kinetic Analysis.

Kinetic equations were modeled in Mathcad 15 or Sigmaplot version 12.5 and fit to experimental data using the latter.

RESULTS AND DISCUSSION

Developing a Kinetic Scheme for Reactions at E_4(4H).

A simplified version of the LT kinetic scheme for N_2 fixation that focuses on electron accumulation and centrally important *re/oa* equilibrium is shown in scheme A of Figure 3. It includes delivery of four e^-/H+ to form E_4(4H), with the hydrogenase-like side reaction, formation of H_2 through HP, in states E_n (*n* = 2–4), *and* the catalytic re of H_2 with N_2 binding by E_4(4H) to generate the diazene-level intermediate, E_4(2N2H) (Figure 2). The

Author Manuscript Author Manuscript Author Manuscript Author Manuscript

subsequent formation of two NH_3 molecules through accumulation of an additional 4 equiv by E_4(2N2H) is represented as a single overall process with a composite rate constant (k_{cat}). Following the strategy we developed in studying electrochemical H_2 production,[38] depicted in scheme B of Figure 3, we capture the essence of kinetic scheme A, the competition between nitrogenase on one hand acting "simply" as a hydrogenase through electron accumulation starting at E_0 with H_2 production by HP at E_2(2H) and E_4(4H) and on the other performing its function of N_2 fixation through "capture" of E_4(4H) by N_2 binding/H_2 *re* and release, to generate E_4(2N2H), which irreversibly proceeds to generate two NH_3 molecules. Scheme B omits the reaction in which E_4(4H) is regenerated through *oa* of H_2 by E_4(2N2H) with N_2 liberation (Figure 2), as being negligible in our measurements, because the partial pressures of H_2 generated are so small. This approach is confirmed by a detailed analysis presented in the Supporting Information.

Scheme B in turn can be mapped onto scheme C under steady-state turnover conditions. When E_0 is formed either by HP at E_2(2H) or by NH_3 formation, it is promptly rereduced to E_2(2H), so the E_0-forming processes are instead treated as "directly" generating E_2(2H). In this mapping, the rate constant for electron accumulation (k_{ac}) is a composite representative of the processes of electron delivery by Fe protein to MoFe protein, while the NH_3-producing catalytic rate constant (k_{cat}) in the final step of the cycle is to be understood as a composite corresponding to addition of six e^-/H^+ per N_2 reduced, four involved in NH_3 formation by reduction of diazene-level intermediate E_4(2N2H) and two more associated with the prompt reduction to E_2(2H) of resting state E_0 formed upon release of the second of two NH_3 molecules (compare scheme C with schemes A and B). Finally, liberation of H_2 by E_2(2H) without a change in state reflects HP at E_2(2H) and rapid return of E_0 thus formed to E_2(2H).

Considering the behavior of E_2(2H) more closely, every time it is generated, it is reduced to E_4(4H) with rate constant k_{ac}, with a probability $f_{ac} = k_{ac}/(k_{ac} + k_{HP})$, or liberates H_2 with a rate constant k_{HP}, with a probability $f_{HP} = k_{HP}/(k_{ac} + k_{Hp})$. High-flux conditions may then be defined as occurring when the rate of electron delivery during electron accumulation (rate constant k_{ac}) is much greater than that for the competing H_2 production by HP (rate constant k_{HP}) at states E_n (n = 2 or 3) in scheme A, namely $f_{HP} \rightarrow 0$ in schemes B and C, leading to catalytic behavior according to scheme D, in which all reaction occurs at E_4(4H).

Such a high-flux condition is achievable, despite the fact that the overall electron-delivery process is well-known to be slow,[17] because of a peculiarity in nitrogenase function. As reported by Lowe and Thorneley, after delivery of an electron from the Fe protein, H_2 can only be released from free MoFe protein, namely after the oxidized Fe protein dissociates and before another reduced Fe protein binds.[27] As a result, the competition between the release of H_2 from free MoFe protein and conversion to the next higher E_n state is governed by the rate of binding of a reduced Fe protein to the MoFe protein. With high concentrations of reduced Fe protein relative to MoFe protein (high flux), this rate is increased to the point that reduced Fe protein binds to MoFe protein rapidly compared to the rate of release of H_2 by MoFe protein. As a consequence, states E_n (n = 2 and 3) do not release H_2 by the HP process, and instead, the states "before" E_4(4H) E_n ($n < 4$) progressively accept (e^-/H^+) until they are converted to E_4(4H). This state then reacts, either by HP or by the re process. As a

Author Manuscript Author Manuscript Author Manuscript Author Manuscript

result, the enzyme under high flux, as described by scheme D, behaves in a fashion not, to the best of our knowledge, noted previously: H_2 production at electron-accumulation stages, E_n ($n \leq 3$) is suppressed during turnover as these states become depopulated in favor of an E_4-level state, either E_4(4H) or E_4(2N2H) depending on the partial pressure of N_2; although E_0 is regenerated by N_2 fixation, under high flux it is promptly returned to E_2(2H). In short, during catalysis, the enzyme effectively cycles between the two E_4 states and the little-populated E_2(2H), and thus, kinetic scheme C evolves into truncated scheme D. In this report, we validate scheme C and confirm that high-flux conditions convert it into scheme D.

It is centrally important that, although in steady-state experiments described by schemes C and D, k_{ac} and k_{cat} are composite rate constants, rate constants k_{HP} and k_{re} correspond precisely to the rate constants for reaction of E_4(4H) in scheme A and, indeed, in the full LT scheme. Moreover, the beauty of high-flux, steady-state experiments (scheme D) is that they emphasize the role of E_4(4H) as the 'Janus' intermediate, which acts as a catalytic "branch point" that reacts through one of two channels. It can "fall back" in a "hydrogenase- like" catalytic cycle, releasing H_2 by the first-order HP process (rate constant k_{HP}) without further electron accumulation, regenerating E_2(2H), or it can be "captured" by second-order reaction with N_2 (rate constant k_{re}) with accompanying release of H_2 formed by *re*, to produce E_4(2N2H), which irreversibly proceeds to generate two NH_3 molecules with composite rate constant k_{cat}. High-flux experiments thus provide precision measurements of the centrally important mechanistic rate constants that define the E_4(4H) branch point: k_{HP} and k_{re}.

Kinetic Analysis.

As shown in the Supporting Information, according to schemes C and D, during steady-state turnover the differential equations for the rates of formation of H_2 and NH_3 and loss of N_2 are zero-order in time, and the rates of NH_3 formation/N_2 loss and of H_2 formation can be written as shown in eq 2

$$\frac{\mathrm{dNH_3}}{\mathrm{d}t} = -2\frac{\mathrm{dN_2}}{\mathrm{d}t} \xrightarrow{\mathrm{SS}} k_{\mathrm{NH_3}} \cdot E_0^0 \quad \frac{\mathrm{dH_2}}{\mathrm{d}t} \xrightarrow{\mathrm{SS}} k_{\mathrm{H_2}} E_0^0 \qquad (2)$$

where E_0^0 is the total enzyme concentration. As a result, the total formation of NH_3/loss of N_2 and the formation of H_2 during a turnover experiment are simply proportional to their respective rate constants. The rate constants for the production of the NH_3 product and loss of N_2 for schemes C and D are given by eq 3 where the numerical factor ($1/4$) converts eq 2 to the rate of NH_3 formation per electron, according to the stoichiometry of eq 1. The maximum velocity for NH_3 production is set by the equation $\bar{k} = k_{cat}k_{ac}/(k_{cat} + k_{ac})$, whose form causes it to equal the smaller of the two rate constants, k_{ac} and k_{cat}. The bracketed term in eq 3 has the form

Author Manuscript Author Manuscript Author Manuscript Author Manuscript

$$k_{NH3} = 2k_{N2} \xrightarrow{SS} \left(\frac{1}{4}\right)\frac{\left(k_{re}P_{N2}\right)}{\left(1+\left(\frac{k_{HP}}{k_{ac}}\right)\right)+\frac{\left(k_{re}P_{N2}\right)}{\bar{k}}} \qquad \boxed{\bar{k} = \frac{k_{ac}k_{cat}}{k_{ac}+k_{cat}}}$$

$$= \left(\frac{1}{4}\right)\frac{\left(k_{re}^{z}P_{N2}\right)}{1+\frac{\left(k_{re}^{z}P_{N2}\right)}{\bar{k}}} \begin{cases} \nearrow \left(\frac{1}{4}\right)\left(k_{re}^{z}P_{N2}\right); & P_{N2}\to 0 \\ \searrow \left(\frac{1}{4}\right)\bar{k} & ;\ P_{N2}\to\infty \end{cases} \qquad \boxed{k_{re}^{z} = \frac{k_{re}}{\left(1+\left(\frac{k_{HP}}{k_{ac}}\right)\right)} \quad \frac{k_{HP}}{k_{ac}}\to 0 \xrightarrow{} k_{re}} \qquad (3)$$

$$= \left(\frac{1}{4}\right)\bar{k}\left[\frac{\frac{\left(k_{re}^{z}P_{N2}\right)}{\bar{k}}}{1+\frac{\left(k_{re}^{z}P_{N2}\right)}{\bar{k}}}\right] = \left(\frac{1}{4}\right)\bar{k}\left[\frac{K_{a}^{z}P_{N2}}{1+K_{a}^{z}P_{N2}}\right] \qquad \boxed{K_{a}^{z} = \frac{k_{re}^{z}}{\bar{k}}}$$

of a binding isotherm, with the apparent binding constant equaling the ratio $K_{\mathrm{a}}{}^{z} = k_{re}{}^{z}/\bar{k}$. We allow for variations in flux, namely the rate constant ratio, $z = k_{\mathrm{HP}}/k_{\mathrm{ac}} > 0$ and thus variations in HP at the $E_2(2H)$ state, but have simplified the appearance of the equation by defining the apparent rate constant, $k_{re}{}^{z}$, in terms of the true k_{re} and z, as indicated. For the sake of completeness, we note this equation can be rewritten in the form of a hyperbola or Michaelis-Menten equation (eq 4). The corresponding rate constant for H_2 production for scheme C is presented in eq 5.

$$k_{\mathrm{N}_2} = \left(\frac{1}{2}\right)k_{\mathrm{NH}_3} \xrightarrow[\text{high flux}]{\mathrm{SS}} \left(\frac{1}{8}\right)\frac{v_{\max}P_{\mathrm{N}_2}}{K_{\mathrm{m}}{}^{z}+P_{\mathrm{N}_2}} \qquad (4)$$

$$K_{\mathrm{m}}{}^{z} = \frac{1}{K_{\mathrm{a}}{}^{z}};\ v_{\max} = \bar{k}$$

$$k_{H2} \xrightarrow{SS} \frac{1}{2}\left[\frac{k_{HP}\left(1+\left(\frac{k_{HP}}{k_{ac}}\right)\right)+\left(\frac{1}{4}\right)\left(1+4\left(\frac{k_{HP}}{k_{ac}}\right)\right)\left(k_{re}P_{N2}\right)}{\left(1+\left(\frac{k_{HP}}{k_{ac}}\right)\right)+\frac{\left(k_{re}P_{N2}\right)}{\bar{k}}}\right] \qquad (5)$$

$$= \frac{1}{2}\left[\frac{k_{HP}+\left(\frac{1}{4}\right)\left(1+4\left(\frac{k_{HP}}{k_{ac}}\right)\right)\left(k_{re}^{z}P_{N2}\right)}{1+\frac{\left(k_{re}^{z}P_{N2}\right)}{\bar{k}}}\right] \begin{cases} \nearrow \left(\frac{1}{2}\right)k_{HP}\,;\ P_{N2}\to 0 \\ \searrow \left(\frac{1}{8}\right)\bullet\bar{k}\ ;\ P_{N2}\to\infty \end{cases}$$

Author Manuscript Author Manuscript Author Manuscript Author Manuscript

When $P_{N_2} \rightarrow 0$, H_2 is produced solely by HP with a rate constant $^1/_2\ k_{HP}$ (per electron). At a high P_{N_2}, H_2 is produced solely by the *re* process, at a rate equaling the rate of consumption of N_2; HP at E_2(2H) is associated with the terms involving the k_{HP}/k_{ac} ratio in the numerator of the first form of eq 5.

Schemes B and C and the resultant steady-state turnover rate constants provide a clear mathematical formulation of the competition at the E_4(4H) branch point between the first-order process of H_2 formation by HP without N_2 binding and the second-order *re* process in which the binding and reduction of one N_2 accompanies the *re* of one H_2. This ability of a second-order process to outcompete a first-order one is most clearly captured by taking the ratio of the rate constants for production of H_2 (eq 3) and N_2 consumption (eq 4), denoted *r*, which can be written as shown in eq 6. According to eq 6, at

$$r = \frac{k_{H2}}{k_{N2}} = 2\frac{k_{H2}}{k_{NH3}} \xrightarrow{SS} \left[\frac{k_{HP} + \left(\frac{1}{4}\right)\left(1 + 4\left(\frac{k_{HP}}{k_{ac}}\right)\right)\left(k_{re}^{z} P_{N2}\right)}{\left(\frac{1}{4}\right)\left(k_{re}^{z} P_{N2}\right)}\right] \begin{cases} \frac{4}{\left(k_{re}^{z} P_{N2}\right)} \rightarrow \infty; & P_{N2} \rightarrow 0 \\ \left(1 + 4\left(\frac{k_{HP}}{k_{ac}}\right)\right); & P_{N2} \rightarrow \infty \end{cases} \tag{6}$$

$$= \left[\frac{1 + \left(\frac{1}{4}\right)\left(1 + 4\left(\frac{k_{HP}}{k_{ac}}\right)\right)\left(\frac{k_{re}^{z}}{k_{HP}}\right) P_{N2}}{\left(\frac{1}{4}\right)\left(\frac{k_{re}^{z}}{k_{HP}}\right) P_{N2}}\right] \qquad \boxed{\rho = \left(\frac{k_{re}}{k_{HP}}\right)}$$

$$= \left[\frac{1 + \left(\frac{1}{4}\right)\left(1 + 4\left(\frac{k_{HP}}{k_{ac}}\right)\right) \bullet \rho P_{N2}}{\left(\frac{1}{4}\right) \bullet \rho P_{N2}}\right]$$

low values of P_{N_2}, the rate of H_2 production by HP from E_4(4H) becomes independent of P_{N_2} as $P_{N_2} \rightarrow 0$, while the rate of N_2 consumption, through reductive elimination and production of H_2 and two NH_3 molecules, falls in proportion to P_{N_2}. Hence, as $P_{N_2} \rightarrow 0$, the ratio *r* approaches infinity. At the other extreme, as P_{N_2} increases so that *re* of H_2 with N_2 consumption becomes much faster than HP at E_4(4H), $k_{re}P_{N_2} \gg k_{HP}$, the ratio *r* tends toward a limiting value that depends on the extent of H_2 formation at the E_2(2H) stage of scheme C, which increases with the value of k_{HP}/k_{ac} (eqs 5 and 6). If turnover is in the high-flux limit, $k_{HP}/k_{ac} \rightarrow 0$, there is no HP at the E_2(2H) state, scheme C evolves into scheme D, and these

Author Manuscript Author Manuscript Author Manuscript Author Manuscript

equations predict that the limiting value at high P_{N_2} is $r = 1$. HP at $E_2(2H)$ is abolished, and HP at $E_4(4H)$ is totally outcompeted by N_2 binding with *re* and release of H_2. One H_2 is liberated as one N_2 binds and is reduced to two NH_3 molecules.

Turnover of Nitrogenases.

Figure 4 presents a plot of the specific activities for NH_3 production at equal concentrations of Mo-nitrogenase and Fe-nitrogenase as a function of the partial pressure of N_2 $\left(P_{N_2}\right)$ overlaid by the fits of these two data sets to eq 3. It is noteworthy that the apparent binding affinity constant, $K_a = k_{re}/\bar{k}$, and the maximum velocity $\bar{k}$ obtained in the fits to the specific activities for Fe-nitrogenase (Table 1) are 4- and 10-fold smaller, respectively, than for Mo-nitrogenase. Figure 5 overlays the measurements of r as a function of P_{N_2} for all three nitrogenases with the fits to eq 6. Table 1 lists the parameters derived from the fits for both Mo- and Fe-nitrogenases, including k_{re}, k_{HP}, $\bar{k}$, and the value for the central parameter of catalysis, the ratio of reaction rate constants at the E_4 level, $\rho = k_{re}/k_{HP}$.

With a focus on the behavior of Mo-nitrogenase, consider the ratio r (Figure 5). The fit to eq 6 yields as the ratio of the rate constants for HP and for electron accumulation $z = k_{HP}/k_{ac} = 0$, which implies that the experiments are indeed performed under high-flux conditions, with HP fully suppressed at early stages of electron accumulation, E_n ($n < 4$), and that scheme D applies: both the reaction with N_2 with correlated H_2 production and the HP of H_2 are described by the intrinsic rate constants associated with reactions of $E_4(4H)$, k_{re} and k_{HP}, respectively.

To test this analysis and conclusion, we performed a suite of experiments in which the electron flux is varied at a fixed P_{N_2}. As noted above, the competition between formation of H_2 through HP at E_2 or E_3 and conversion to the next higher E_n state is expressed in the ratio $z = k_{HP}/k_{ac}$ and is governed by the rate of binding of a reduced Fe protein to the MoFe protein. This influence may be incorporated into the description of r through a decrease in z with increasing flux, $z = a[\text{MoFe}]/[\text{Fe}]$, where the parameter, a, is a scale-factor that relates the two ratios. Equation 6, the ratio of product-formation rate constants, r, can then be rewritten in terms of this relationship (also see, SI), (eq 7).

$$r = \frac{k_{H2}}{k_{N2}} = \left[\frac{1 + \left(\frac{1}{4}\right)\left(1 + 4\left(a \bullet \frac{[MFe]}{[Fe]}\right)\right) \bullet \rho P_{N2}}{\left(\frac{1}{4}\right) \bullet \rho P_{N2}}\right] \quad \boxed{z = \frac{k_{HP}}{k_{ac}} = a \bullet \frac{[MFe]}{[Fe]}} \tag{7}$$

The plots of eq 7 in Figure 6 illustrate how, in the high-flux regime, where $z \ll 1$, the ratio r is invariant with flux as expected, while as z increases and the system falls out of this regime, r increases. This measured ratio of H_2/N_2 as a function of the MoFe protein/Fe protein ratio shown in Figure 6 is consistent with an earlier study.[39]

Author Manuscript Author Manuscript Author Manuscript Author Manuscript

For Mo-nitrogenase, the measured dependence of r on [MoFe]/[Fe] at $P_{N_2} = 1$ atm is captured with precision by eq 7 using the corresponding values of ρ and a (Table 1). The data show that Mo-nitrogenase reaches the high-flux regime when [MoFe]/[Fe] ≳ 1, while our experiments in Figures 4 and 5 were performed at [MoFe]/[Fe] = 1/20! This finding shows that scheme D indeed is appropriate for analysis of our experiments, with z → 0, that the apparent rate constant for *re* obtained by combining the parameters from the fits to the P_{N_2} titration (Figure 4) with rate ratio r (Figure 5) (k_{re}^{z}, eq 3) is precisely the intrinsic value, k_{re}, that describes the *re* process of E_4(4H), and, finally, that rate constant k_{HP} is precisely the value for E_4(4H).

With this foundation, the plots in Figure 5, the "H_2/N_2" ratio, r, are shown to be a remarkable demonstration of the power of the present approach to reveal the kinetic basis for the different catalytic efficiencies of the alternative nitrogenases. The key difference is expressed in the ratio of reaction rate-constants at the E_4 level, $\rho = k_{re}/k_{HP}$, which captures the tendency for the E_4(4H) intermediate to undergo the *re* process with H_2 release upon N_2 binding and, ultimately, NH_3 formation (second-order rate constant, k_{re}), instead of producing H_2 by HP (first-order rate constant, k_{HP}). Equation 6 shows that ρ alone controls this branching at E_4(4H), and the plots of r as a function of P_{N_2} for the two nitrogenases, which so beautifully overlay the data, are generated through the use of eq 6 merely by adjusting this single parameter (Table 1).

Viewed from a different perspective, these measurements and their description by eq 6 clearly demonstrate that activation of E_4(4H) for N_2 binding indeed occurs through *re* and release of H_2. This coupling between N_2 binding and the release of H_2, which was first incorporated in the LT kinetic scheme, is highlighted in scheme D and, as visualized through the plot of r versus P_{N_2} in Figure 5, both predicts and provides an explanation for the experimental finding that an extremely high P_{N_2} does not entirely suppress H_2 formation by Mo-nitrogenase but instead leads asymptotically to the formation of one H_2 per formation of two NH_3 molecules per reduction of one N_2.[28] For $P_{N_2} = 50$ atm, eq 6 yields an r value of 1.02 for Mo-nitrogenase, essentially reproducing the Burris value of r (1.13 ± 0.13).

With this analysis and the resulting parameters in hand, we can quantify the remark made above that under high flux all the electron accumulation stages, E_n ($n \leq 3$), become depopulated in favor of an E_4-level state. According to this analysis, in these high-flux experiments, [MoFe]/[Fe] = 1/20, one calculates that ~99% of the cofactor is present in the E_4 state, as either E_4(4H) or E_4(2N2H), with the relative amounts depending on P_{N_2}. Moreover, direct calculation with the full scheme A gives an equivalent result.

Focusing next on Fe-nitrogenase, we find the measured flux dependence of the ratio r at $P_{N_2} = 1$ plotted in Figure 6 shows that this enzyme also operates in the high-flux regime in our measurements. Fe-nitrogenase reaches the high-flux regime when [FeFe]/[Fe] ≳ 1,

Author Manuscript Author Manuscript Author Manuscript Author Manuscript

whereas our experiments in Figures 4 and 5 were performed at a far smaller ratio ([FeFe]/[Fe] = 1/30). Thus, here too, all catalytic reactions occur at the E_4(4H) state, and its catalytic properties captured in the reaction rate constants can be straightforwardly compared to those of Mo-nitrogenase through the kinetic analysis of the turnover experiments.

Comparison of the parameters derived from the N_2 consumption titration for Fe-nitrogenase (Figure 4) and the H_2/N_2 titration (Figure 5) with those of Mo-nitrogenase (Table 1) reveals that the major functional difference between the Mo- and Fe-nitrogenases is associated with rate constant k_{re} for H_2 *re*/N_2 binding by E_4(4H). The k_{re} for Mo-nitrogenase is 10-fold greater than that of Fe-nitrogenase, while the asymptotic maximum rate constant for N_2 reduction, proportional to $\bar{k}$, is twice as big. As a result, the apparent affinity constant for N_2, $K_a = k_{re}/\bar{k}$, is 4-fold greater for Mo-nitrogenase than for Fe-nitrogenase.

The higher H_2 production by the Fe-nitrogenase is best considered in terms of the N_2/H_2 ratio. The fits to the data in Figure 5 show that the k_{re}/k_{HP} ratio, which captures the tendency of E_4(4H) to undergo *re* rather than HP, is 7-fold larger for Mo-nitrogenase than for Fe-nitrogenase. Even though the value of k_{HP} determined for MoFe is indeed slightly higher than that for Fe-nitrogenase, because the Mo-nitrogenase value of k_{re} is 10-fold higher, there is a 7-fold greater preference for *re* instead of HP (rate ratio, ρ) for Mo-nitrogenase than for Fe-nitrogenase. Finally, even though Fe-nitrogenase is thus a considerably poorer N_2 fixation catalyst, because it follows the same mechanism as Mo-nitrogenase, in the high-flux limit that applies here, eq 6 nonetheless predicts that $r \rightarrow 1$ at sufficiently high P_{N_2}; extrapolation of the Fe-nitrogenase curve in Figure 5 to 50 atm predicts an r value of 1.11.

Finally, the V-nitrogenase is widely understood to have catalytic efficacy midway between those of Mo- and Fe-nitrogenases, and the kinetic model developed here can quantify this point using only the single value of the H_2/N_2 ratio at $P_{N_2} = 1$ available in the literature.[4,6,12,30,31] Given the intermediate behavior of V-nitrogenase and the finding that both more and less effective enzymes are in the high-flux regime during *in vitro* turnover, we may assume the same for V-nitrogenase, in which case the predicted curve of r versus P_{N_2} for this enzyme is completely determined by the single parameter ρ, which is fixed by the single value of r at $P_{N_2} = 1$; the resulting curve is plotted on Figure 5. The value of ρ and the curve it specifies indeed lie between those for Mo- and Fe-nitrogenase, which quantifies the relative tendency of E_4(4H) to follow its two alternative reaction channels. The ratio for V-nitrogenase relates to those of the other two nitrogenases as k_{re}/k_{HP} (Mo) = 5.1, k_{re}/k_{HP} (V) = 2, and k_{re}/k_{HP} (Fe) = 0.77. In other words, at a given pressure of N_2, V-nitrogenase is ~40% as likely to undergo reaction with N_2 as Mo-nitrogenase and Fe-nitrogenase is only 15% as likely to thus react.

As a final comment about kinetic approaches to nitrogenase function, note that the k_{re}/k_{HP} ratio = 5.1 atm^{-1} derived in this fashion for *A. vinelandii* Mo-nitrogenase is of far higher precision but is satisfyingly similar to the ratio of rate constants measured by LT as refined by Wilson and Watt[32] for a different Mo-nitrogenase, k_{re}/k_{HP} = 3.4 atm^{-1} (conversion of

Author Manuscript Author Manuscript Author Manuscript Author Manuscript

their k_{re} in units of M^{-1} s^{-1} used a Henry's law constant K of 6.1×10^{-4} M/atm).[40] However, the benefits of the approach presented here are highlighted by the remark by Wilson and Watt that the value they report for k_{HP} is "subject to error of a factor of approximately 2" whereas the key kinetic constants in Table 1 have errors of <10%. And, of course, the focused ability to compare the catalytically important rate constants associated with E_4(4H) among the three nitrogenases that is introduced by the current approach is entirely new.

CONCLUSIONS

The work reported here provides a kinetic analysis of nitrogenase reactivity that focuses on reaction at the catalytically central E_4 state and precisely describes observed H_2 production and N_2 consumption/NH_3 production under steady-state turnover conditions. The measurements as analyzed with the new kinetic model provide unprecedented insight into the catalytic behavior of the E_4(4H) 'Janus' intermediate, whose differing properties in the three nitrogenases give rise to their differing catalytic efficacy. Although electron transfer to the catalytic MFe proteins from the Fe protein is rate-limited by P_i release,[17] analysis of the measurements shows that across a wide range of electron fluxes introduced by varying the protein concentration ratio, [MFe]/[Fe], the nitrogenase behaves in a fashion that had not been recognized previously: H_2 production is suppressed at the electron accumulation stages, E_n ($n < 3$), and during catalysis, the enzyme effectively cycles between the two states at the E_4 level and the little populated E_2(2H), as is captured by the truncated cycle of scheme D. We note that the ratio of MoFe protein to Fe protein measured inside the cell ([MoFe]/[Fe] = $^1/_2$) corresponds to "high-flux" conditions (Figure 6), which means that the present measurements reproduce the enzyme's behavior *in vivo*.[41] It is significant that the ratio of nitrogenase component proteins inside the cell is small enough to minimize the wasteful H_2 formation by HP that would occur at concentration ratios greater than unity, yet at the same time, the ratio is not made even smaller, to no appreciable functional benefit, by the presence of excess Fe protein; the cell does not make more Fe protein than is necessary. This is of considerable physiological benefit, as protein production is a significant energy demand on the cell. It should be noted that Fe protein is also involved in the assembly of both of the metalloclusters contained with the MoFe protein, P-cluster, and FeMo-cofactor.[42] However, the amount of Fe protein required to sustain these functions under steady-state growth conditions is likely to be minimal, indicating that the elevated level of Fe protein relative to MoFe protein within cells represents a physiologically relevant mechanism for maximizing catalytic efficiency.

The results further support the earlier findings that suggested that unlimited high pressures of N_2 could not completely suppress H_2 production and that the ratio of H_2 production to N_2 consumption in fact approaches unity at high pressures,[28] behavior explained by the *re/oa* mechanism we have developed recently.[9,18–20] The kinetic analysis shows how this behavior arises: the second-order process of enzyme activation by H_2 *re* with liberation through N_2 binding outcompetes the first-order "decay" of E_4(4H) through the HP process.

Two striking differences in the function of Mo-, V-, and Fe-nitrogenases are revealed here. Most importantly, the observation that Fe-nitrogenase produces far more H_2 per N_2 reduced

Author Manuscript Author Manuscript Author Manuscript Author Manuscript

at $P_{N_2} \leq 1$ atm than the Mo-enzyme arises not, as might have been expected, because Fe-nitrogenase exhibits a correspondingly greater rate constant for HP. Indeed, the rate constant for HP by E_4(4H) of Fe-nitrogenase is only 70% of that for Mo-nitrogenase! Instead, Mo-nitrogenase is a more efficient catalyst for N_2 reduction because of the roughly 10-fold greater second-order rate constant for the N_2-fixing pathway of E_4(4H) reactivity, resulting in a k_{re}/k_{HP} rate constant ratio of ~7 (Table 1): Mo-nitrogenase is simply a better N_2 reduction catalyst. Second, the maximum velocity for NH_3 formation, $\bar{k}$, for Mo-nitrogenase is 2 times that of Fe-nitrogenase, a finding reinforced by previous data demonstrating that electron flux through Mo-nitrogenase is roughly twice that of Fe-nitrogenase. These two differences account for the poorer catalytic efficiency of Fe-nitrogenase and can be extrapolated to the intermediate reactivity observed for V-nitrogenase.

An experimental and theoretical study of the differences among the nitrogenases will provide a fruitful avenue for improving our understanding of how the differences in the metal clusters and their surrounding protein environments tune the reactivity to favor N_2 reduction over H_2 evolution in the different forms of nitrogenase, as quantified by the kinetic analysis presented here.

Supplementary Material

Refer to Web version on PubMed Central for supplementary material.

Acknowledgments

Funding

Support was provided by the U.S. Department of Energy, Office of Science, Basic Energy Sciences, via Grants DE-SC0010687 and DE-SC0010834 to L.C.S. and D.R.D., and the National Science Foundation, via Grant MCB 1515981to B.M.H.

ABBREVIATIONS

BSA	bovine serum albumin
FeFe-co	active-site cofactor of iron-only nitrogenase
FeMo-co	active-site cofactor of molybdenum-dependent nitrogenase
Fe-N_2ase	iron-only nitrogenase
FeV-co	active-site cofactor of vanadium-dependent nitrogenase
HP	hydride protonolysis
$\bar{k}$**,**	turnover number (kcat)
K	binding constant for N2 (kre/$\bar{k}$)
kac	rate constant for accumulation of electrons on a cofactor
kcat	turnover number

Author Manuscript Author Manuscript Author Manuscript Author Manuscript

kHP	rate constant for hydride protonolysis
kre	rate constant for reductive elimination
LT	Lowe and Thorneley kinetic scheme
Mo-N2ase	molybdenum-dependent nitrogenase
oa	oxidative addition
P_{N_2},	partial pressure of dinitrogen
r	k_{H_2}/k_{N_2}
re	reductive elimination
V-N2ase	vanadium-dependent nitrogenase
z	kHP/kac

REFERENCES

(1). Raymond J, Siefert JL, Staples CR, and Blankenship RE (2004) The natural history of nitrogen fixation. Mol. Biol. Evol 21, 541–554. [PubMed: 14694078]

(2). Burris RH, and Roberts GP (1993) Biological nitrogen fixation. Annu. Rev. Nutr 13, 317–35. [PubMed: 8369149]

(3). Gruber N, and Galloway JN (2008) An Earth-system perspective of the global nitrogen cycle. Nature 451, 293–296. [PubMed: 18202647]

(4). Eady RR (1996) Structure-function relationships of alternative nitrogenases. Chem. Rev 96, 3013–3030. [PubMed: 11848850]

(5). Burgess BK, and Lowe DJ (1996) Mechanism of molybdenum nitrogenase. Chem. Rev 96, 2983–3012. [PubMed: 11848849]

(6). Hu Y, Lee CC, and Ribbe MW (2012) Vanadium nitrogenase: A two-hit wonder? Dalton Trans. 41, 1118–1127. [PubMed: 22101422]

(7). Robson R, Woodley P, and Jones R (1986) Second gene (nifH) coding for a nitrogenase iron protein in Azotobacter chroococcum is adjacent to a gene coding for a ferredoxin-like protein. EMBO J. 5, 1159–1163. [PubMed: 15966103]

(8). Joerger RD, Jacobson MR, Premakumar R, Wolfinger ED, and Bishop PE (1989) Nucleotide sequence and mutational analysis of the structural genes (anfHDGK) for the second alternative nitrogenase from Azotobacter vinelandii. J. Bacteriol 171, 1075–1086. [PubMed: 2644222]

(9). Hoffman BM, Lukoyanov D, Yang Z-Y, Dean DR, and Seefeldt LC (2014) Mechanism of nitrogen fixation by nitrogenase: The next stage. Chem. Rev 114, 4041–4062. [PubMed: 24467365]

(10). Fay AW, Blank MA, Lee CC, Hu Y, Hodgson KO, Hedman B, and Ribbe MW (2010) Characterization of isolated nitrogenase FeVco. J. Am. Chem. Soc 132, 12612–12618. [PubMed: 20718463]

(11). Krahn E, Weiss B, Krockel M, Groppe J, Henkel G, Cramer S, Trautwein A, Schneider K, and Muller A (2002) The Fe-only nitrogenase from *Rhodobacter capsulatus*: identification of the cofactor, an unusual, high-nuclearity iron-sulfur cluster, by Fe K-edge EXAFS and ^{57}Fe Mossbauer spectroscopy. JBIC, J. Biol. Inorg. Chem 7, 37–45. [PubMed: 11862539]

(12). Hales BJ (1990) Alternative nitrogenase. Adv. Inorg. Biochem 8, 165–198. [PubMed: 2206026]

(13). Sippel D, and Einsle O (2017) The structure of vanadium nitrogenase reveals an unusual bridging ligand. Nat. Chem. Biol 13, 956–960. [PubMed: 28692069]

Author Manuscript Author Manuscript Author Manuscript Author Manuscript

(14). Peters JW, Fisher K, Newton WE, and Dean DR (1995) Involvement of the P-cluster in intramolecular electron transfer within the nitrogenase MoFe protein. J. Biol. Chem 270, 27007–27013. [PubMed: 7592949]

(15). Chan JM, Christiansen J, Dean DR, and Seefeldt LC (1999) Spectroscopic evidence for changes in the redox state of the nitrogenase P-cluster during turnover. Biochemistry 38, 5779–5785. [PubMed: 10231529]

(16). Danyal K, Dean DR, Hoffman BM, and Seefeldt LC (2011) Electron transfer within nitrogenase: evidence for a deficitspending mechanism. Biochemistry 50, 9255–9263. [PubMed: 21939270]

(17). Yang Z-Y, Ledbetter R, Shaw S, Pence N, Tokmina-Lukaszewska M, Eilers B, Guo Q, Pokhrel N, Cash VL, Dean DR, Antony E, Bothner B, Peters JW, and Seefeldt LC (2016) Evidence that the P_i release event is the rate-limiting step in the nitrogenase catalytic cycle. Biochemistry 55, 3625–3635. [PubMed: 27295169]

(18). Lukoyanov D, Khadka N, Yang Z-Y, Dean DR, Seefeldt LC, and Hoffman BM (2016) Reversible photoinduced reductive elimination of H2 from the nitrogenase dihydride state, the E4(4H) Janus intermediate. J. Am. Chem. Soc 138, 1320–1327. [PubMed: 26788586]

(19). Lukoyanov D, Khadka N, Yang Z-Y, Dean DR, Seefeldt LC, and Hoffman BM (2016) Reductive elimination of H2 activates nitrogenase to reduce the N≡N triple bond: characterization of the E4(4H) Janus intermediate in wild-type enzyme. J. Am. Chem. Soc 138, 10674–10683. [PubMed: 27529724]

(20). Lukoyanov D, Yang Z-Y, Khadka N, Dean DR, Seefeldt LC, and Hoffman BM (2015) Identification of a key catalytic intermediate demonstrates that nitrogenase is activated by the reversible exchange of N_2 for H_2. J. Am. Chem. Soc 137, 3610–3615. [PubMed: 25741750]

(21). Rohde M, Sippel D, Trncik C, Andrade SLA, and Einsle O (2018) The critical E_4 state of nitrogenase catalysis. Biochemistry, DOI: 10.1021/acs.biochem.8b00509.

(22). Spatzal T, Perez KA, Einsle O, Howard JB, and Rees DC (2014) Ligand binding to the FeMo-cofactor: structures of CO-bound and reactivated nitrogenase. Science 345, 1620–1623. [PubMed: 25258081]

(23). Sippel D, Rohde M, Netzer J, Trncik C, Gies J, Grunau K, Djurdjevic I, Decamps L, Andrade SLA, and Einsle O (2018) A bound reaction intermediate sheds light on the mechanism of nitrogenase. Science 359, 1484–1489. [PubMed: 29599235]

(24). Raugei S, Seefeldt LC, and Hoffman BM (2018) A critical computational analysis illuminates the reductive-elimination mechanism that activates nitrogenase for N_2 reduction. Proc. Natl. Acad. Sci. U. S. A,.

(25). Lukoyanov D, Yang Z-Y, Barney BM, Dean DR, Seefeldt LC, and Hoffman BM (2012) Unification of reaction pathway and kinetic scheme for N_2 reduction catalyzed by nitrogenase. Proc. Natl. Acad. Sci. U. S. A 109, 5583–5587. [PubMed: 22460797]

(26). Thorneley RN, and Lowe DJ (1983) Nitrogenase of *Klebsiella pneumoniae*. Kinetics of the dissociation of oxidized iron protein from molybdenum-iron protein: identification of the rate-limiting step for substrate reduction. Biochem. J 215, 393–403. [PubMed: 6316927]

(27). Thorneley RNF, and Lowe DJ (1985) Kinetics and mechanism of the nitrogenase enzyme In Molybdenum Enzymes (Spiro TG, Ed.) pp 221–284, Wiley-Interscience Publications, New York.

(28). Simpson FB, and Burris RH (1984) A nitrogen pressure of 50 atm does not prevent evolution of hydrogen by nitrogenase. Science 224, 1095–1097. [PubMed: 6585956]

(29). Harris DF, Lukoyanov DA, Shaw S, Compton P, Tokmina-Lukaszewska M, Bothner B, Kelleher N, Dean DR, Hoffman BM, and Seefeldt LC (2018) Mechanism of N_2 reduction catalyzed by Fe-nitrogenase involves reductive elimination of H_2. Biochemistry 57, 701–710. [PubMed: 29283553]

(30). Eady RR, Robson RL, Richardson TH, Miller RW, and Hawkins M (1987) The vanadium nitrogenase of *Azotobacter chroococcum*. Purification and properties of the VFe protein. Biochem. J 244, 197–207. [PubMed: 2821997]

(31). Schneider K, and Muller A (2004) Iron-only nitrogenase: Exceptional catalytic, structural and spectroscopic features In Catalysts for Nitrogen Fixation, pp 281–307, Springer, Dordrecht, The Netherlands.

Author Manuscript Author Manuscript Author Manuscript Author Manuscript

(32). Wilson PE, Nyborg AC, and Watt GD (2001) Duplication and extension of the Thorneley and Lowe kinetic model for *Klebsiella pneumoniae* nitrogenase catalysis using a MATHEMATICA software platform. Biophys. Chem 91, 281–304. [PubMed: 11551440]

(33). Christiansen J, Goodwin PJ, Lanzilotta WN, Seefeldt LC, and Dean DR (1998) Catalytic and biophysical properties of a nitrogenase apo-MoFe protein produced by an *nifB*-deletion mutant of *Azotobacter vinelandii*. Biochemistry 37, 12611–12623. [PubMed: 9730834]

(34). Burgess BK, Jacobs DB, and Stiefel EI (1980) Large- scale purification of high activity *Azotobacter vinelandii* nitrogenase. Biochim. Biophys. Acta 614, 196–209. [PubMed: 6930977]

(35). Peters JW, Fisher K, and Dean DR (1994) Identification of a nitrogenase protein-protein interaction site defined by residues 59 through 67 within the *Azotobacter vinelandii* Fe protein. J. Biol. Chem 269, 28076–28083. [PubMed: 7961744]

(36). Corbin JL (1984) Liquid chromatographic-fluorescence determination of ammonia from nitrogenase reactions: A 2-min assay. Appl. Environ. Microbiol 47, 1027–1030. [PubMed: 16346533]

(37). Barney BM, Igarashi RY, Dos Santos PC, Dean DR, and Seefeldt LC (2004) Substrate interaction at an iron-sulfur face of the FeMo-cofactor during nitrogenase catalysis. J. Biol. Chem 279, 53621–53624. [PubMed: 15465817]

(38). Khadka N, Milton R, Shaw S, Lukoyanov D, Dean DR, Minteer SD, Raugei S, Hoffman BM, and Seefeldt LC (2017) Mechanism of nitrogenase H_2 formation by metal-hydride protonation probed by mediated electrocatalysis and H/D isotope effects. J. Am. Chem. Soc 139, 13518–13524. [PubMed: 28851217]

(39). Wherland S, Burgess BK, Stiefel EI, and Newton WE (1981) Nitrogenase reactivity: effects of component ratio on electron flow and distribution during nitrogen fixation. Biochemistry 20, 5132–5140. [PubMed: 6945871]

(40). Sander R (2015) Compilation of Henry's law constants (version 4.0) for water as solvent. Atmos. Chem. Phys 15, 4399–4981.

(41). Poza-Carrion C, Jimenez-Vicente E, Navarro-Rodriguez M, Echavarri-Erasun C, and Rubio LM (2014) Kinetics of *nif* gene expression in a nitrogen-fixing bacterium. J. Bacteriol 196, 595–603. [PubMed: 24244007]

(42). Jimenez-Vicente E, Yang Z-Y, Ray WK, Echavarri-Erasun C, Cash VL, Rubio LM, Seefeldt LC, and Dean DR (2018) Sequential and differential interaction of assembly factors during nitrogenase MoFe protein maturation. J. Biol. Chem 293, 9812–9823. [PubMed: 29724822]

Author Manuscript Author Manuscript Author Manuscript Author Manuscript

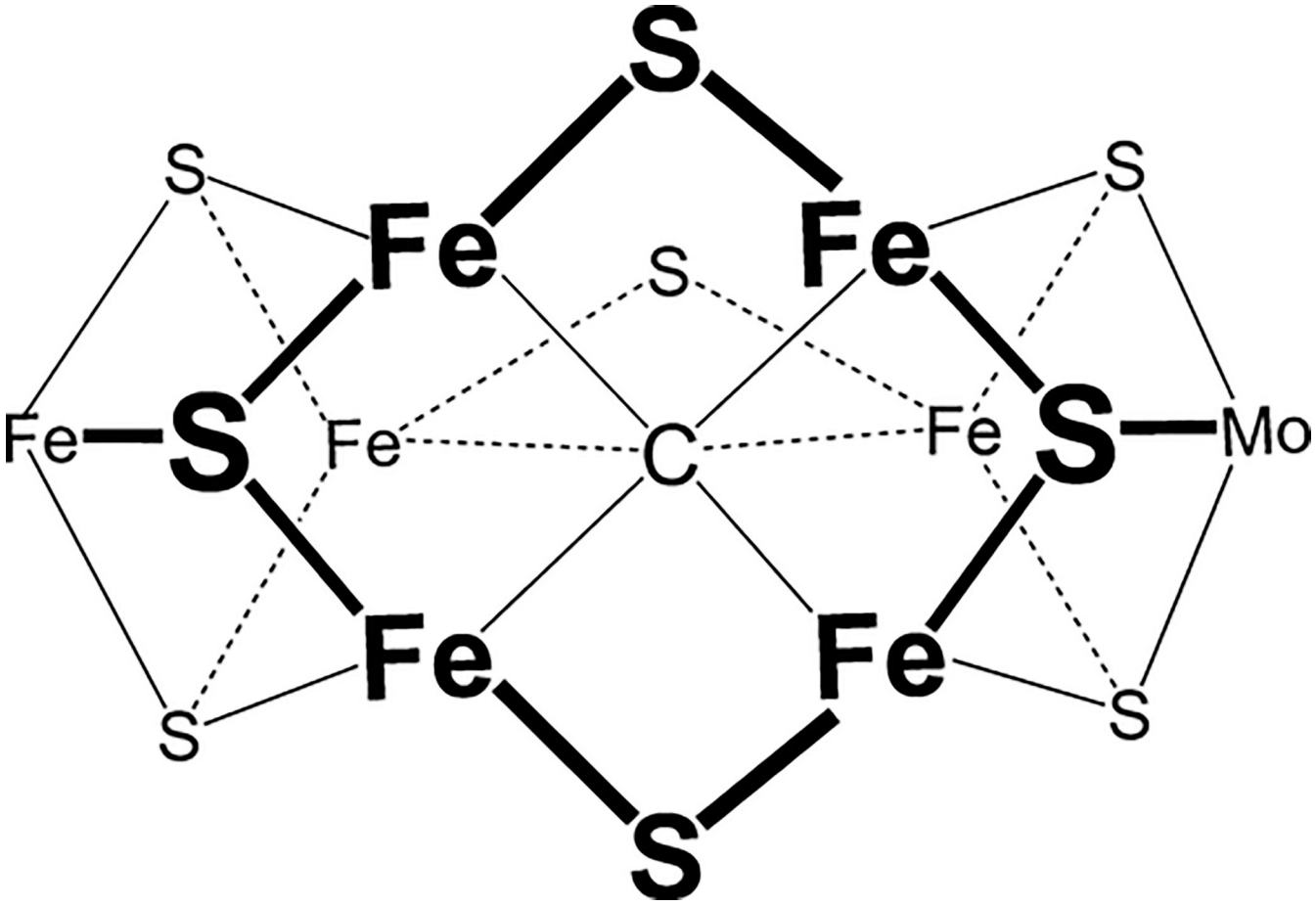

Figure 1.
Structure of the core of the FeMo-cofactor, looking down on the Fe2,3,6,7 face.

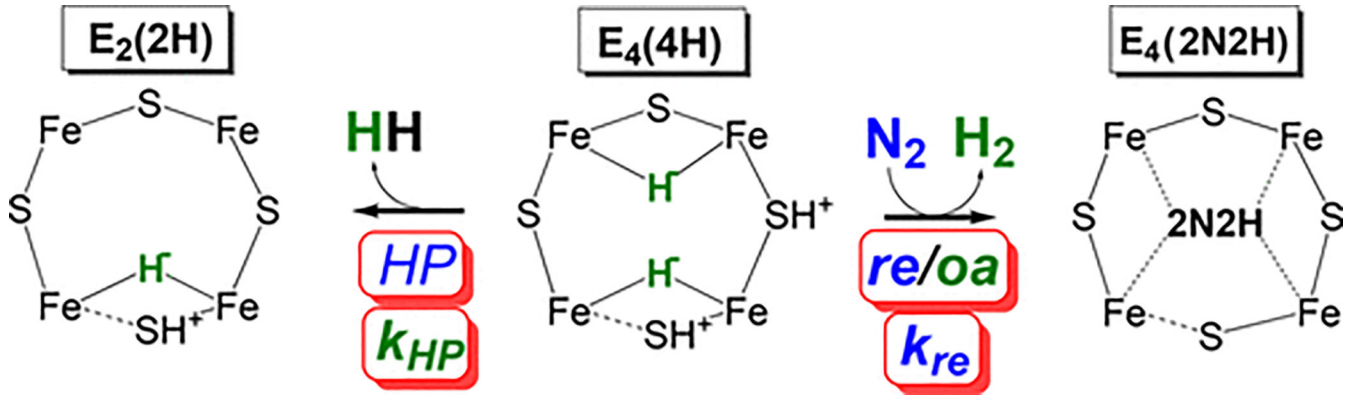

Figure 2.

Reactions of the E_4 state. The $E_4(4H)$ state (center) is shown relaxing to the left by hydride protonolysis (HP) to generate $E_2(2H)$ with rate constant k_{HP} or reacting with N_2 to the right through the reductive elimination/oxidative addition *(re/oa)* equilibrium that activates nitrogenase to break the N≡N bond. Although this process is an equilibrium, the *oa* of H_2 is not significant in our experiments (see the Supporting Information), so only the "forward", re rate constant, k_{re}, is shown. Note that the positioning of hydrides and protons is a matter of current interest, with plausible alternative possibilities; for the sake of concreteness, our own current best guess is shown, also noting the possible lability of an Fe–S bond with a dotted line. "2N2H" denotes a diazene-level intermediate.[9]

Author Manuscript Author Manuscript Author Manuscript Author Manuscript

Author Manuscript Author Manuscript Author Manuscript Author Manuscript

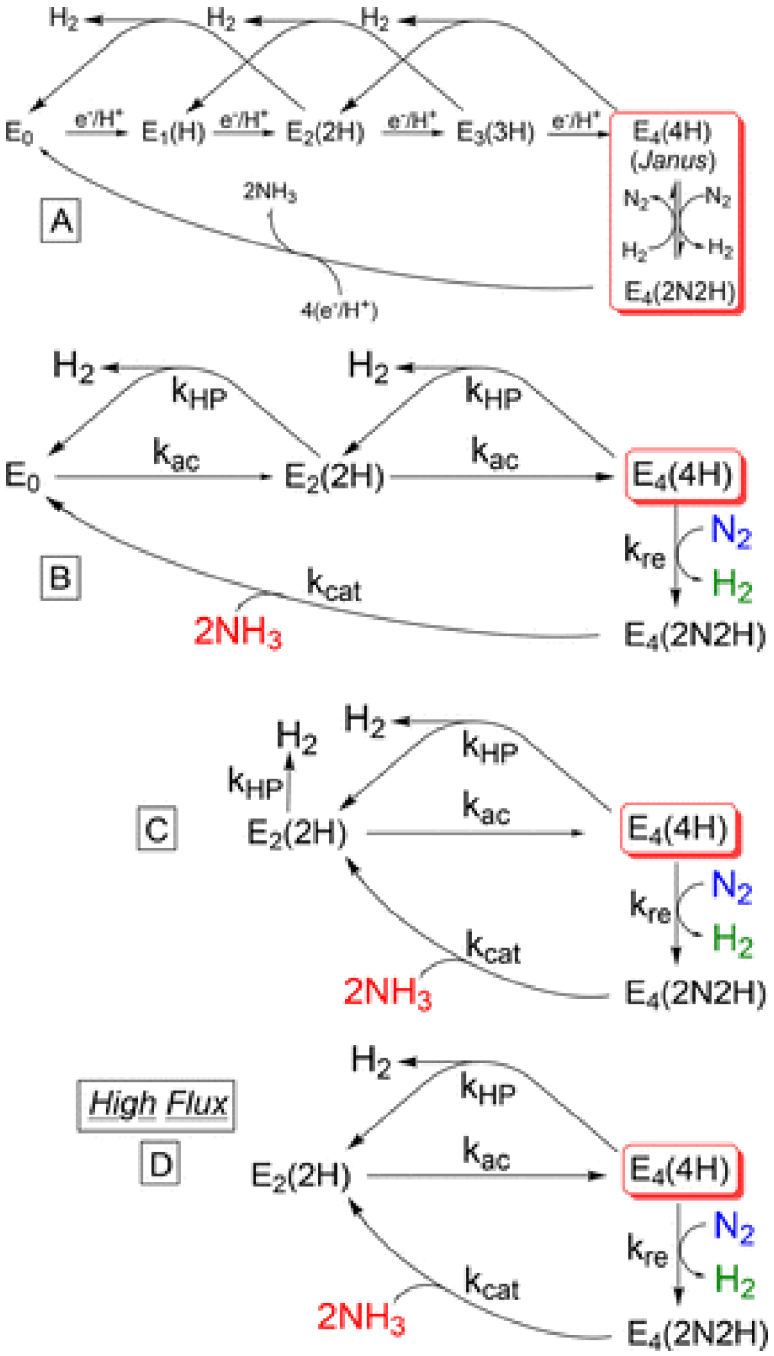

Figure 3.

As described in the text, scheme A is a simplified LT kinetic scheme for N_2 fixation; its essence is captured by scheme B. This scheme in turn is further simplified under high-flux, steady-state turnover conditions to scheme C, which evolves into truncated kinetic scheme D.

Author Manuscript Author Manuscript Author Manuscript Author Manuscript

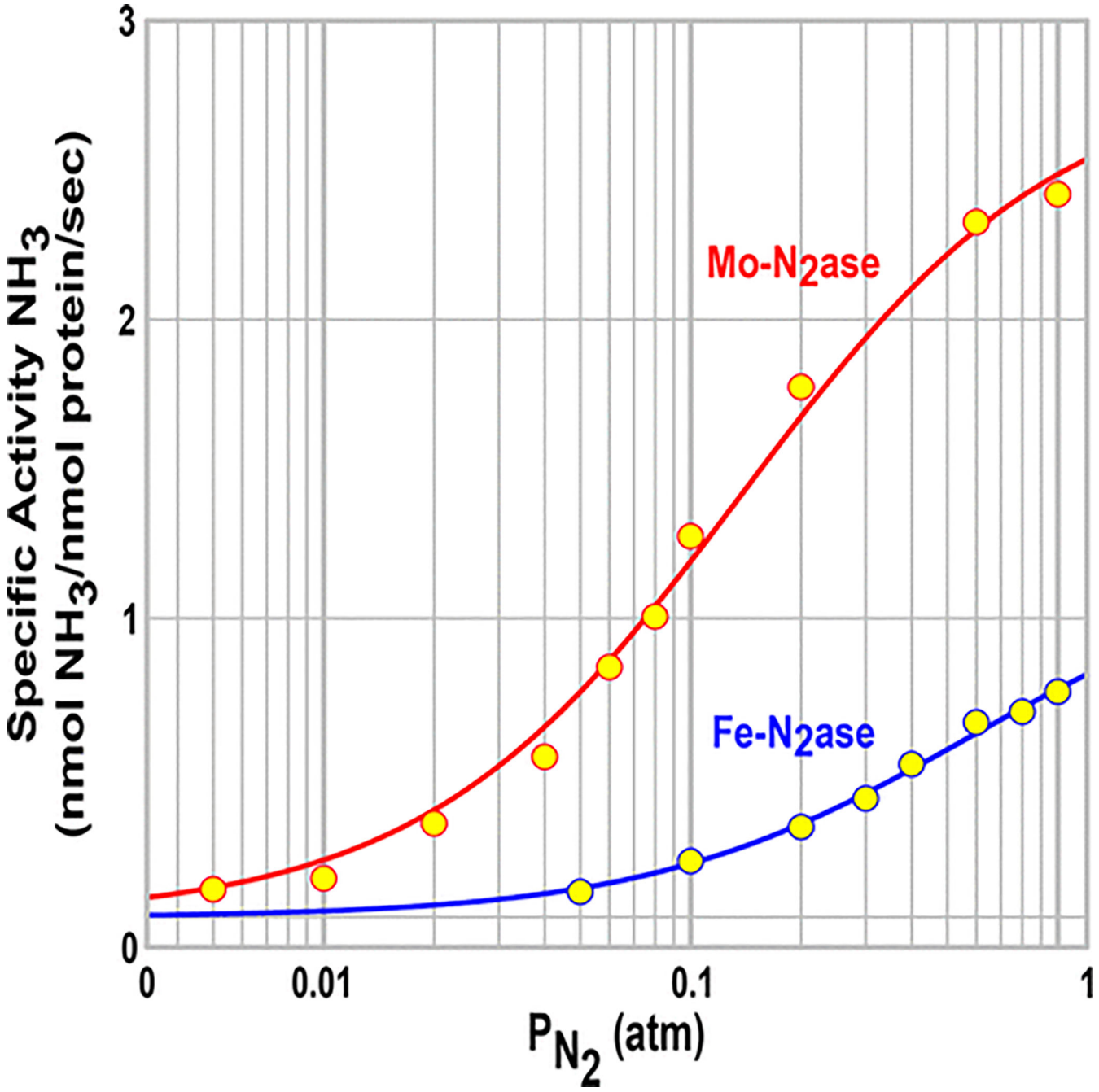

Figure 4.

Specific activities for NH_3 formation by Mo- and Fe-nitrogenases as a function of the partial pressure of N_2. Overlaid are fits to eq 3 obtained with SigmaPlot; values of k_{re} and K_a for MoFe (red trace) and FeFe (blue) are listed in Table 1. Assays were performed as described in Materials and Methods.

Author Manuscript Author Manuscript Author Manuscript Author Manuscript

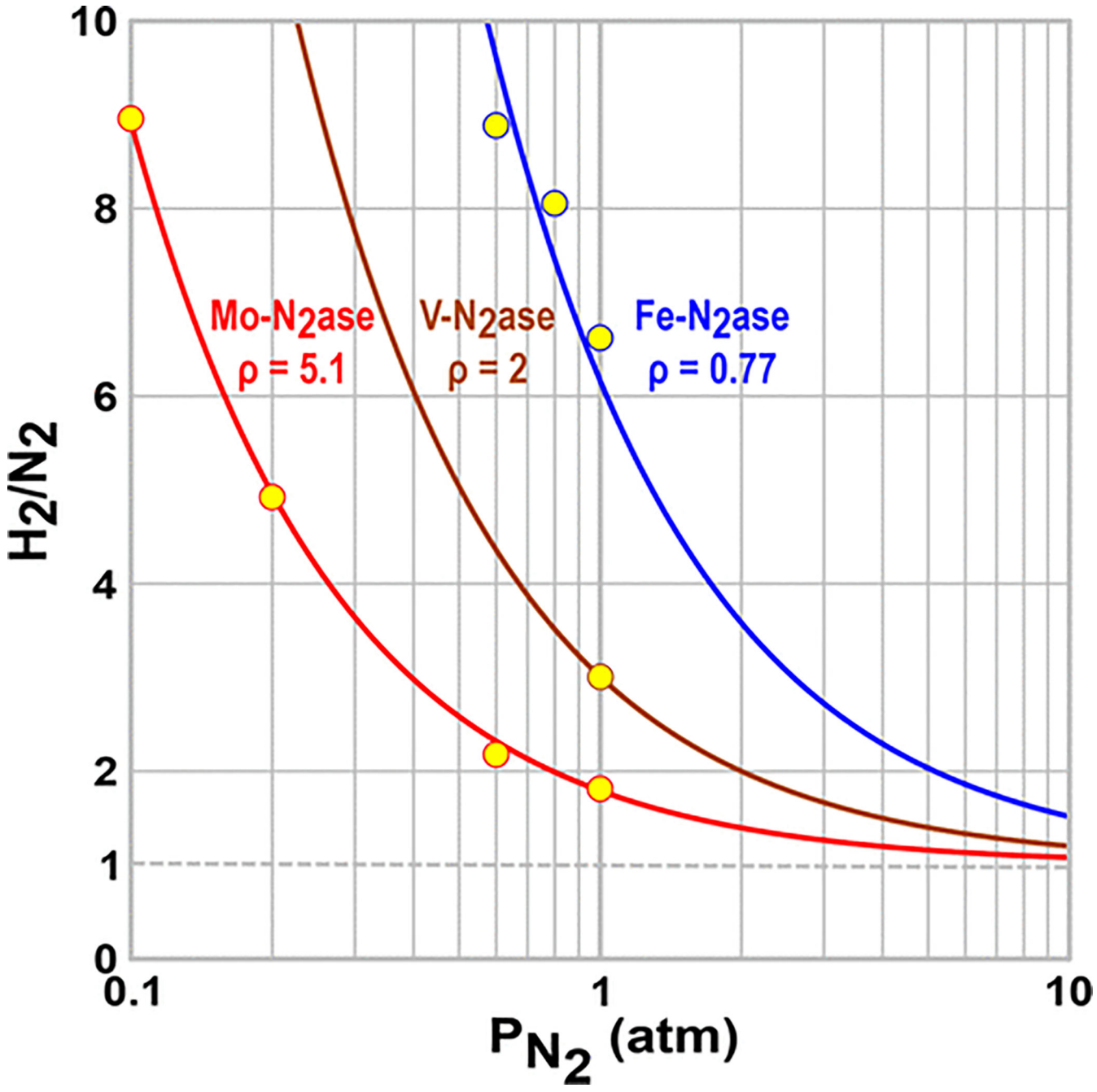

Figure 5.

Ratio of H_2 formed to N_2 consumed as a function of the partial pressure of N_2 for Mo-nitrogenase (red) and Fe-nitrogenase (blue). Overlaid are fits to eq 6 using SigmaPlot. Values of $\rho = k_{re}/k_{HP}$ are listed in Table 1. Assays were performed as described in Materials and Methods.

Author Manuscript Author Manuscript Author Manuscript Author Manuscript

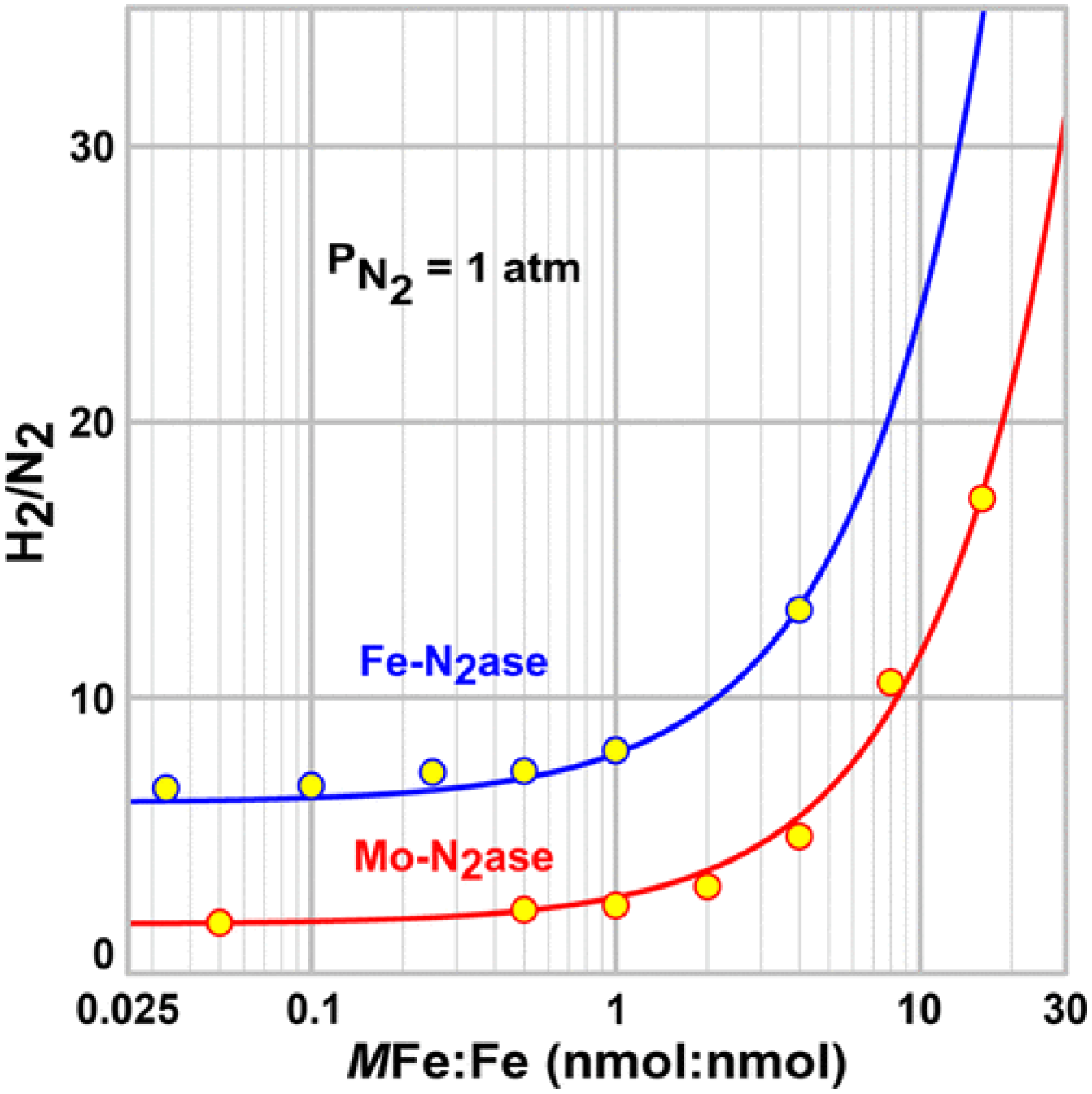

Figure 6.

Ratio of H_2 formed to N_2 consumed as a function of flux ([MFe:Fe], where M = Mo or Fe) for Mo-nitrogenase (red) and Fe-nitrogenase (blue). Traces were determined by fixing ρ to the value in Table 1 and fitting parameter a in eq 7 using SigmaPlot (Table 1). Assays were performed as described in Materials and Methods.

Author Manuscript Author Manuscript Author Manuscript Author Manuscript

Table 1.

Kinetic Parameters Obtained from High-Flux Turnover

	$\rho = k_{re}/k_{HP}$ $(atm^{-1})^a$ (*r* fit)	k_{re} $(s^{-1}\ atm^{-1})^b$ (*y*)	$K_a = k_{re}/\bar{k}$ $(atm^{-1})^b$ (*z*)	k_{HP} $(s^{-1})^c$ (calcd)	$\bar{k}(s^{-1})^c$ (calcd)	a^d
Mo	5.1 (1)	83 (5)	7.3 (5)	16.3	11.3	0.22
Fe	0.77 (5)	8.5 (5)	1.8 (2)	11	4.7	0.19
Mo/Fe	6.6	9.8	4.1	1.5	2.4	

[a] Obtained from fits in Figure 5.

[b] Obtained from fits in Figure 4.

[c] Calculated from other parameters.

[d] Obtained from fits in Figure 6.

Biochemistry. Author manuscript; available in PMC 2019 April 11.